Stratospheric Aerosol Measurements I: Time Variations at Northern Midlatitudes

D. J. HOFMANN, J. M. ROSEN, T. J. PEPIN AND R. G. PINNICK

Department of Physics and Astronomy, University of Wyoming, Laramie 82070

(Manuscript received 13 September 1974, in revised form 18 February 1975)

ABSTRACT

The results of over 70 balloon soundings, by the University of Wyoming's Atmospheric Physics Group mostly during 1972 and 1973 from a number of stations, are being utilized in a study of the temporal and spatial distribution of the global stratospheric aerosol. This paper deals with the instrumentation, calibration, etc., and with the results of monthly soundings from the Laramie (41°N) station during the approximately two-year period of measurement. This period comprises an interval apparently free of major volcanic activity just prior to the extensive volcanic contributions to the stratospheric aerosol which occurred in late 1974. It thus may be compared to the pre-Agung era and is perhaps as close to the so-called "natural stratospheric background conditions," if indeed such conditions ever exist, as will likely be attained in the near future.

A simple seasonal variation in the total stratospheric aerosol loading below about 20 km altitude dominates the temporal variation at Laramie, resulting in a maximum in winter and a minimum in summer. A high correlation with tropopause height is observed. The seasonal variation appears to be superimposed on a long-term variation, the nature of which is unknown. Above 20 km, no seasonal variation is evident, and the natural aerosol production processes appear to be nearly in equilibrium with loss processes.

1. Introduction

Although the stratospheric aerosol layer was discovered by Junge over a decade ago (Junge *et al.*, 1961), only recently has there been sufficient interest in this subject to pursue further identification and study of this phenomenon on a noticeable scale. This interest has been spawned by general concern over the possible climatic effects of small particle buildup in the stratosphere. Thus a sizable number of research groups are addressing this problem by a variety of techniques in order to identify the nature and source of the stratospheric aerosol, its temporal behavior, and the mode of global transport of this material.

Most of the recent efforts to measure the stratospheric aerosol have made use of improvements or extensions of previously used methods such as optical radar (lidar), impactor sampling, and balloon-borne optical particle counters. These programs have been reviewed by Hofmann (1974) and the earlier measurements have been reviewed by Rosen (1969, 1972) and Cadle (1972). There appears to be general agreement that a worldwide submicron-size aerosol layer exists in the 20 km altitude range, that the concentration of particles in this layer has generally decreased in the past ten years, and that during this period the concentration was largely composed of the sulfate ion, probably in the form of sulfuric acid. There is considerably less agreement or, for that matter, data concerning such characteristics as seasonal variations, global distributions, or sources and sinks.

The research reported here involves measurement of the stratospheric aerosol with a particle counter that measures light scattered by single aerosol particle *in situ*. The instrument was designed for stratospheric application and was first flown in the stratosphere by one of the authors about ten years ago (Rosen, 1964) and was later used to measure the stratospheric aerosol at a number of different latitudes (Rosen, 1968).

The research program at the University of Wyoming through which these data have been collected is a program of global scope in the sense that data have been obtained from eleven stations ranging in latitude from 85°N to 90°S. Balloon soundings from most of the stations were conducted on a bimonthly basis. One exception to this is the Laramie station, from which monthly soundings have been conducted since early in 1972. In this paper, the first of a series dealing with the results of the research program, the instrumentation will be described, the detector characteristics and calibration discussed in detail, and the results from the Laramie soundings presented. These results form the basis for a temporal study of the stratospheric aerosol at northern midlatitudes over a period of approximately two years.

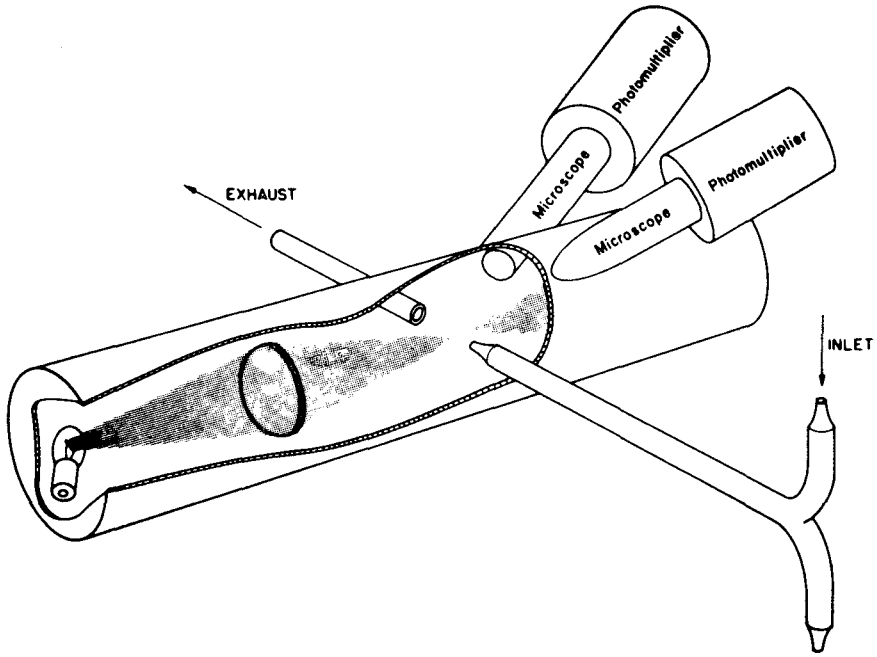

FIG. 1. Schematic diagram of the aerosol detector.

2. Description of instrumentation

The aerosol detector currently in use in this program is an updated, lightweight version of that first used by Rosen in 1963. Because its present configuration and weight (~9 kg) are in the radiosonde class, it has been referred to as a "dustsonde." Fig. 1 shows the detector in schematic form. Air being sampled is pumped at a rate of about $\frac{3}{4}$ ℓ min^{-1} in a well-defined stream through the focal point of the condenser lens in the 2500 cm^3 scattering chamber where individual particles scatter light into the microscopes. The optical system permits collection of light scattered 8° through 38° from the direction of forward scattering, with a maximum collection efficiency at about 25°. The light pulses are detected by photomultiplier tubes, the outputs of which are size-discriminated. The requirement of simultaneous pulses from both photomultipliers enhances the signal-to-noise ratio, noise being due mainly to Rayleigh scattering from air molecules at low altitude, and scattering from the chamber walls and cosmic ray scintillation in the photomultiplier glass at high altitude. Such background elimination precautions are necessary since for the smallest particles (~0.25 μm effective diameter) only a few photons are scattered into the field of view of the instrument.

The background counting rate is measured about every 15 min during flight by slightly pressurizing the scattering chamber with clean air. Thus the background, which varies with altitude since it is caused mostly by Rayleigh scattering from air molecules, may be subtracted from the total counting rate. The background for most instruments is essentially zero above about 10 km.

The air sample flow rate, after correction for pressure differences due to balloon rise rate and the low outside temperature, is then used to calculate the aerosol concentration. At the presently observed low stratospheric particle concentrations (~1 particle cm^{-3} with diameter $\gtrsim$0.3 μm), the counting rate of the instrument for these particles in the stratosphere is of the order of 10 counts per second. With a balloon rise rate of 5 m s^{-1}, an average of 100 particles are registered every 50 m. To reduce statistical fluctuation, 500 particles are counted for each data point so that the average vertical resolution at the current low concentrations is about 250 m, or about 100 data points per sounding from ground level to 27 km for the >0.3 μm diameter particles.

Although the integral concentrations of as many as five sizes have been measured on a single flight by pulse-height discrimination, the standard detector system measures only two integral sizes. The discriminators are generally calibrated to register particles having diameters $\gtrsim$0.3 μm and $\gtrsim$0.5 μm. These sizes are based on an index of refraction of 1.40. The practical upper size limit, due to gravitational settling in the intake tube, is about 5 μm diameter at stratospheric levels. The calibration technique and related research will be discussed in the next section. Such research suggests that over the usable size range of this detector, and within the time limits of a balloon sounding, two or possibly three different sizes are all that one is justified in measuring.

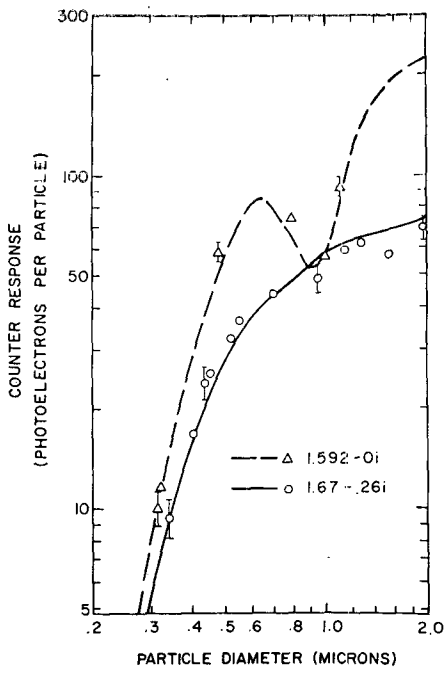

FIG. 2. Photoelectric particle counter response [measured (circles and triangles) and calculated using Mie scattering theory (smooth curves)] for single particles as a function of particle size. Calculated curves have been normalized for best fit to the measured response for polystyrene latex particles with refractive index $m=1.592-0i$.

The sounding vehicle generally employed is a 70,000 ft^3 (50 ft inflated diameter) 0.50 mil plastic balloon. With a total payload of about 16 kg, the altitude capability of such a system is about 27 km, with a rise rate of $\sim$0.3 km min^{-1}. Upon reaching ceiling altitude the parachute is severed from the balloon and descends with the payload averaging approximately 0.5 km min^{-1}, again sampling the atmosphere. Comparison of the aerosol data on ascent and descent allows one to confirm unusual observations. The aerosol measurement is not contaminated by the balloon during ascent as the detector package is lowered following balloon launch by a reel device to a position 90 m below the balloon.

In addition to aerosol concentrations in two size ranges, temperature, pressure, dew point, and ozone concentration are also generally measured on each sounding. All data are telemetered via 1680 MHz radiosonde transmitters so that soundings can be made from any weather station equipped for radiosonde flights.

3. Aerosol detector response and calibration

A detailed report of the response of an aerosol detector identical to that utilized here has been given in the literature (Pinnick *et al.*, 1973) and we will review only the salient features of this work. A method of generating monodisperse (uniform size) spherical aerosol of known index of refraction in the laboratory was developed to study the characteristics of the detector. The aerosol was generated by atomization of a diluted solution of the material to be made into aerosol with a vibrating capillary and allowing evaporation of the volatile solvent prior to measurement with the particle counter. In this manner the response to aerosol of a number of materials having indexes of refraction ranging from nearly that of water to nearly that of carbon was studied, and the results are presented in Figs. 2 and 3. The four materials for which the response is shown in these figures were polystyrene latex (index $=1.592-0i$), nigrosin dye ($1.67-0.26i$), Dow Corning 200 fluid ($1.4033-0i$), and Flowmaster ink ($1.65-0.069i$). The magnitude of the imaginary part of the index of refraction is a measure of the absorptive property of the material. The measured response, in scattered photoelectrons per particle (circles and triangles), was compared to the calculated response (smooth curves), using Lorenz-Mie scattering theory for the particular optical configuration of the instrument. The many different sizes of particles were obtained by varying the solution concentration. Other variables are also important in the vibrating capillary technique, e.g., orifice size and pressure, solvent viscosity, and resonant frequency. The particle size was measured and a high degree of sphericity was verified by electron microscope observation of the particles.

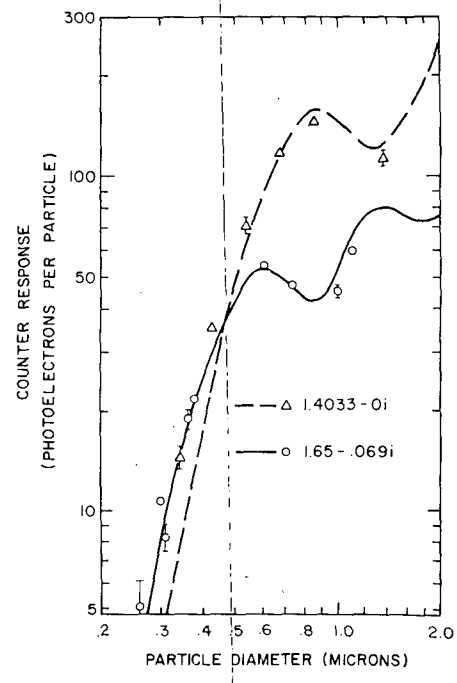

FIG. 3. As in Fig. 2 except for variations in the refractive indexes of the measured particles. Calculated curves have again been normalized for best fit to the measured response for polystyrene latex particles with refractive index $m=1.592-0i$ (see Fig. 2).

TABLE 1. Particle sizes as a function of pulse-height ratio and refractive index

Pulse-height ratio	Particle diameter (μm) Index 1.40	Index 1.50
10	2.70	3.00
1	0.53	0.51
0.1	0.31	0.29
0.05	0.28	0.26
0.025	0.25	0.23

A single normalization was used for all the theoretical curves in Figs. 2 and 3, i.e., a best fit to the measured response for polystyrene latex particles. The double-valued property of the response curve, at least for non-absorbing or slightly absorbing particles, exhibited in Figs. 2 and 3, is characteristic of the scattering properties of particles which have a size comparable to the wavelength of the incident radiation.

Thus having some assurance that the instrument's response for spherical particles was in agreement with accepted theory, it was advantageous to utilize a commercially available polystyrene latex aerosol for calibration, even though its index of refraction (1.592) is somewhat different from the characteristic index thought to be prevalent in the stratosphere (i.e., 1.40, or that of a 75% H_2SO_4, 25% H_2O solution) as determined from stratospheric evaporation measurements by Rosen (1971).

In the actual calibration scheme, a 0.5 μm diameter level discriminator is set and any other levels are determined electronically by fixed ratios. As can be seen in Fig. 3, the 1.4033 index aerosol has a scattering response of about 50 photoelectrons per particle at a particle diameter of 0.5 μm. From Fig. 2 we see that a response of 50 photoelectrons per particle corresponds to a polystyrene latex (index 1.592) particle with a diameter of either 0.45 μm or about 1 μm due to the double-valued property of the response. Thus 1.01 μm polystyrene latex spheres are used in the calibration and the >0.5 μm diameter level discriminators are adjusted until half of the 1.01 μm polystyrene particles are counted by each phototube. (The pulse-height distribution is essentially Gaussian.) The >0.3 μm level is then obtained electronically by a fixed level setting 10 times smaller in pulse height than the >0.5 μm level, as determined by the response measurements mentioned earlier (i.e., about 5 photoelectrons per particle).

The theoretical sizes which we have measured on occasion and corresponding relative pulse heights for refractive indexes of 1.40 and 1.50 are given in Table 1. The pulse-height ratio is defined as the pulse height due to the indicated size particle divided by the pulse height due to 0.5 μm diameter particles. The rapid decrease in pulse, or pulse-height ratio, as one goes to smaller particles is due to the fact that the scattering cross section falls off approximately as the radius to the 6th power in the 0.25–0.5 μm size range.

To discriminate pulses due to particles having a pulse-height ratio of 0.025, extremely low-noise, high-gain phototubes are necessary. Since it was necessary to construct many detectors in this program, it was unfeasible to have such excellent phototubes in all units. Thus from a batch of 50 tubes one might be good enough to obtain the 0.025 ratio, while almost all of them will be capable of the 0.1 ratio. Prior to June 1972 tubes were handpicked to obtain the 0.05 ratio on all flights. With an increasing demand for detectors, we subsequently changed to the 0.1 ratio, requiring a correction to the data obtained prior to June (6 soundings) in order to compare data in a time variation study. This correction was determined by measuring the 1, 0.1 and 0.05 pulse-height ratios simultaneously in the stratosphere on a number of occasions. This experiment suggests that for the present stratospheric aerosol, the 0.05 ratio particles are about 30% higher in concentration than the 0.1 ratio particles. This factor has thus been applied in correcting all data obtained prior to June 1972 for comparison with later data.

Particles with a pulse-height ratio of 10, resulting from very large particles, are not measured routinely since, due to the low concentrations, only 1 or 2 particles per sounding have been detected. The size region between about 0.6 and 1.8 μm is to be avoided due to the double-valued nature of the detector response in this region. Therefore for balloon sounding applications, it appears practical to measure only two or three sizes between 0.25 and 0.50 μm, on a routine basis, with this type of instrument.

In actuality the detector is not 100% efficient in counting particles, owing mainly to photoelectron statistics. The pulse-height distributions of monodisperse aerosol are observed to be essentially Gaussian and the width of these distributions is quite large since relatively few scattered photons are detected for small particles. Thus, with a coincident system, a particle may indicate that it is above a certain size in one phototube output but not in the other, resulting in the need for a correction. From the response to monodisperse aerosol measured in the laboratory, and utilizing a realistic size distribution, it is possible to calculate the efficiency vs size and index of refraction for such a detector (Pinnick and Hofmann, 1973). Table 2 summarizes some of these results.

TABLE 2. Detector efficiency (%) as a function of pulse-height ratio and refractive index.

Pulse-height ratio	Efficiency Index 1.40	Index 1.50
10	94	97
1	95	92
0.1	86	87
0.05	83	84
0.025	81	81

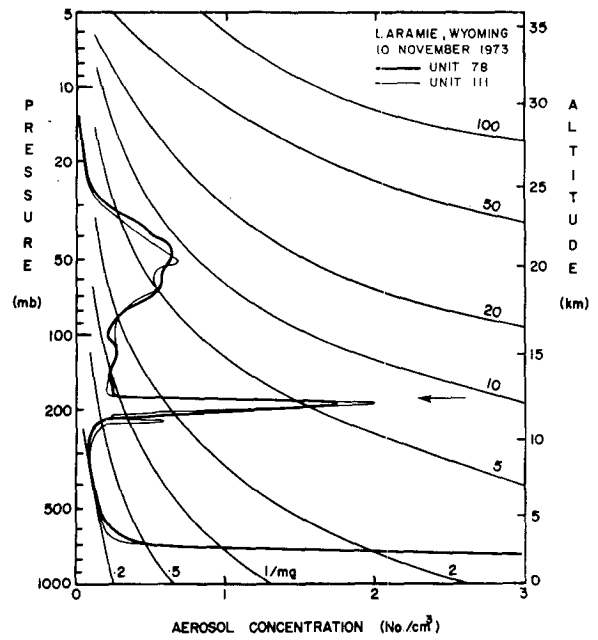

FIG. 4. Comparison of the vertical aerosol profiles obtained by two detectors flown on the same sounding in November 1973. The arrow indicates the observed position of the tropopause and the curved grid lines are lines of constant mixing ratio in units of particles per milligram of air.

4. Discussion of uncertainties

We can identify two classes of uncertainties, those associated with the measured concentration of particles and those associated with the quoted particle size. Each of these classes of uncertainties contain both instrumental errors and uncertainties due to the nature of the particles being measured. The critical variables which affect instrumental errors are the air sample flow rate and the detector response calibration. The important particle characteristics are composition or index of refraction and configuration or size and shape.

From laboratory simulation of balloon ascent, it has been determined that an uncertainty in flow rate of $\pm 5\%$ exists for some instruments depending on the quality of construction of the gear pumps used to draw the air sample through the detector. This uncertainty in flow rate will directly affect the measured concentrations.

For flight-to-flight comparisons, the relative accuracy of the calibration (assuming no change in aerosol composition) is estimated to be within $\pm 5\%$ in terms of pulse height. Since the response varies roughly as the sixth power of the radius in the 0.3 μm diameter size region, the relative size uncertainty is of the order of $\pm 1\%$. Uncertainties in the flight-to-flight discriminator level settings of this magnitude will contribute about $\pm 2\%$ to the uncertainty in the relative measured concentrations of particles with diameters $\geqslant 0.3\,\mu$m as determined from the local size distribution. The same reasoning for the $\geqslant 0.5\,\mu$m diameter particles gives a relative uncertainty of about $\pm 6\%$.

Since each data point in a vertical distribution of the $\geqslant 0.3\,\mu$m diameter particles is computed from a registration of 500 particles, statistical fluctuations are about $\pm 4\%$. For the total integrated stratospheric aerosol (number of particles in a cm^2-column computed for each sounding), such fluctuations are negligible. An overall estimate of the maximum error in measured absolute particle concentrations for the $\geqslant 0.3\,\mu$m diameter particles arising mainly from uncertainties in the flow rate and statistical fluctuations is $\pm 10\%$. For flight-to-flight comparisons, utilizing the total integrated aerosol from different instruments, the uncertainties in flow rate and calibration cause a relative uncertainty of about $\pm 6\%$. For comparisons of the same instrument, this error is reduced to the calibration error alone and is only a few percent.

Concerning variations in the aerosol composition, as stated earlier, most measurements indicate a high relative concentration of the sulphate ion (Lazrus *et al.*, 1971); however, a truly representative index of refraction is not always known unless an impactor is also flown. We have done this on a number of occasions at Laramie using the impactor sampler of the Australian CSIRO group (Bigg *et al.*, 1970, 1971). Analyses of the electron microscope grids from the impactor have indicated the predominance of the sulphate ion on those flights. For calculation purposes, we have used indices of 1.40, 1.50 and $1.50-0.05i$, where the latter index includes an imaginary (absorptive) part. This range of values results in a possible sizing error of $\pm 4\%$. Other possible sources of error such as differences in the flow rate in flight as compared to during calibration, causing a variation in pulse height due to particles passing through the illuminated volume in different times and consequently scattering varying amounts of light, and other uncertainties in the relative calibrations have been considered and are small. Thus an uncertainty of $\pm 5\%$ in particle size for spherical particles is estimated.

Particle shape can have a large effect on the response; however, slightly non-spherical configurations have been investigated in the laboratory and are in reasonable agreement with Mie scattering theory for equivalent volume spheres for scattering into the forward angles which are observed by this detector. Clumping together of particles, as has apparently been observed on occasions in impactor samples by Bigg and Ono (1974), would obviously give misleading results. However, the ratio of concentrations of the two sizes routinely measured has remained uniform and one can say that whatever the configuration, it is probably not changing significantly from flight to flight.

5. Time variations at northern midlatitudes

While measurements have been carried out at most stations on a bi-monthly basis, soundings from the

Laramie station at 41°N have been conducted approximately once a month. This frequency of soundings has proven satisfactory for studying the time variation of the natural aerosol background, at least under the prevailing low concentration conditions encountered.

As an example of a typical aerosol profile, Fig. 4 shows the results of a comparison sounding carried out at Laramie in November 1973. These data and all further data, unless otherwise stated, are for particles with diameters $\gtrsim 0.3\ \mu$m. The arrow in the figure indicates the position of the tropopause and the curved grid lines are lines of constant mixing ratio in units of particles per milligram of air. Two instruments were included in this sounding to check the consistency among different units. The total number of particles determined by the two instruments is in agreement to within a few percent, verifying theoretical predictions of the uncertainties.

The aerosol layer near 20 km in Fig. 4 is the classical Junge layer, while that at about 12 km, just below the tropopause, could be a transient feature, although such aerosol layers near the tropopause are often observed during winter and spring. The size distribution of the latter particles is not drastically different from that in the high layer as indicated by the ratio of concentrations of the two sizes measured ($>0.3\ \mu$m/$>0.5\ \mu$m) shown in Fig. 5, again for both instruments.

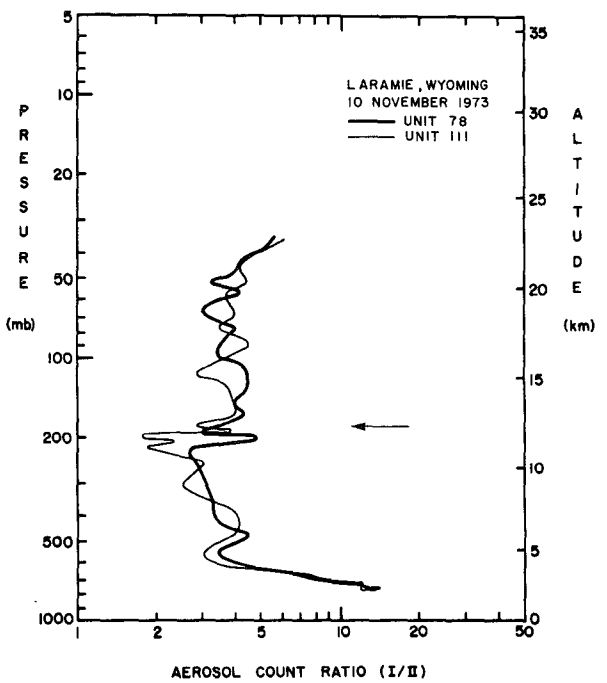

FIG. 5. Comparison of the vertical profiles of the ratio of concentrations of particles ($>0.3\ \mu$m diameter divided by $>0.5\ \mu$m diameter) obtained by two detectors flown on the same sounding in November 1973. The arrow indicates the observed position of the tropopause.

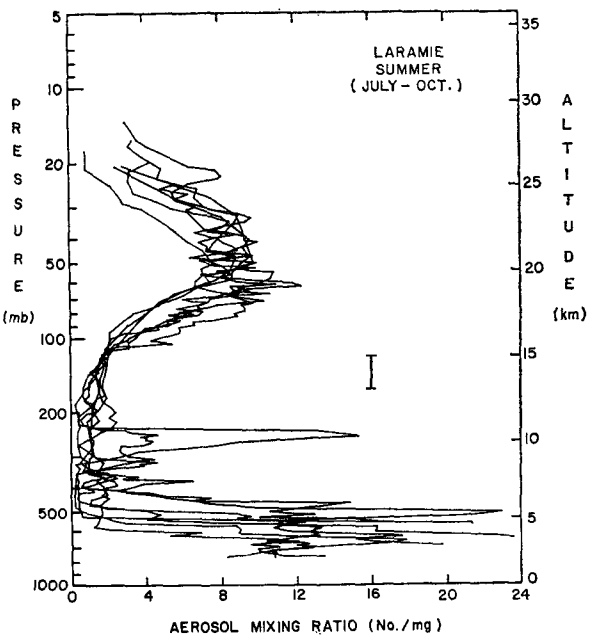

FIG. 6. Summer aerosol mixing ratio height profiles at Laramie, Wyo. The vertical bar marks the observed tropopause positions.

The characteristic seasonal trends of the stratospheric aerosol layer over Laramie are exhibited in Figs. 6, 7 and 8, which show the aerosol mixing ratio (particles mg^{-1} ambient air) vs height for three periods labeled summer (July–October), winter (November–February), and spring (March–June), respectively. These data include soundings through December 1973. The vertical bars in the figures indicate the observed range of tropopause positions for the soundings. Certain features of the aerosol profiles suggested this categorization.

Beginning with Fig. 6, we find the summer aerosol layer to be highly stable with both the upper troposphere and the lower stratosphere relatively free of particles. The high mixing ratio features near 10 km are due to cirrus clouds; their presence can be ascertained by observing the ratio of concentrations of the two sizes of particles measured. The latter are generally characterized by a steeper size distribution (i.e., predominantly smaller particles than observed in the stratosphere).

The winter profiles, in Fig. 7, appear less uniform and as the tropopause decreases in altitude the lower stratosphere appears to increase in particle concentration, generally in a layered fashion near 200 mb pressure (12 km height). Notice, however, that the upper troposphere still maintains relatively low mixing ratios. The high degree of nonuniformity between 20 and 30 km is due in part to an apparent particle increase at high altitude in January 1973 and was present to a lesser degree in February and March. In terms of the number of particles this increase was small but in terms of the

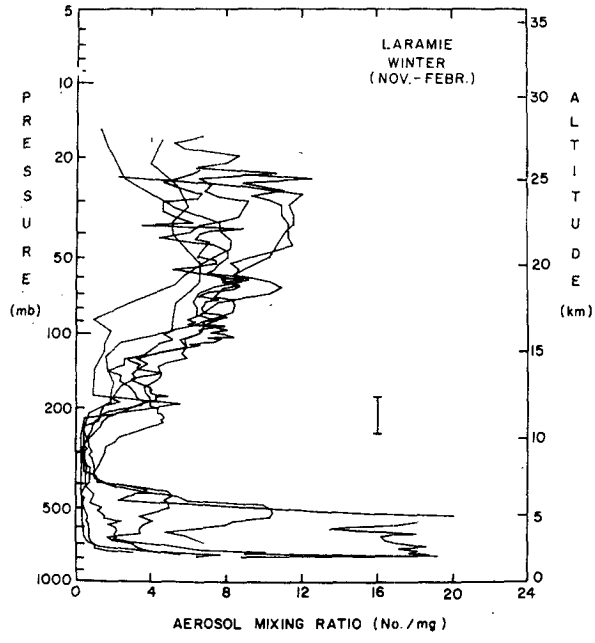

FIG. 7. As in Fig. 6 except for winter.

mixing ratio, at these high altitudes, it was significant.

The spring soundings, shown in Fig. 8, can be characterized as somewhat variable, being highly layered with both the lower stratosphere and the upper troposphere dominated by such laminae of relatively high mixing ratio.

In Fig. 9, the extremes of the seasonal variation are compared, now in terms of particle concentration vs altitude. With this format the winter layered structure

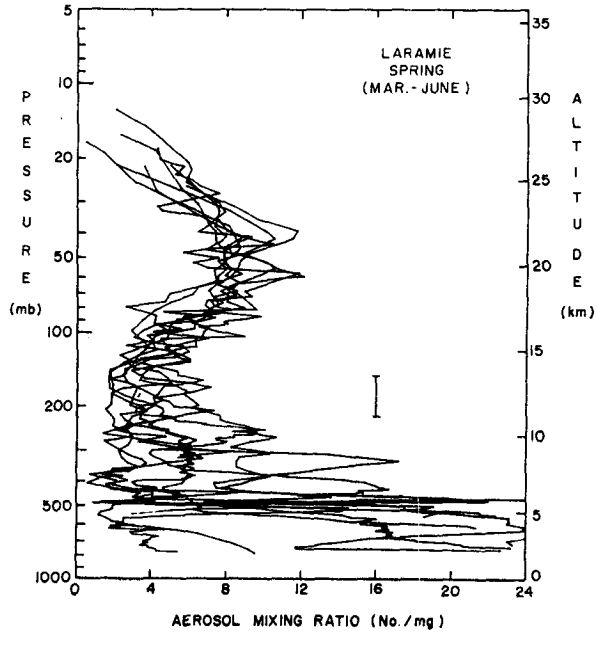

FIG. 8. As in Fig. 6 except for spring.

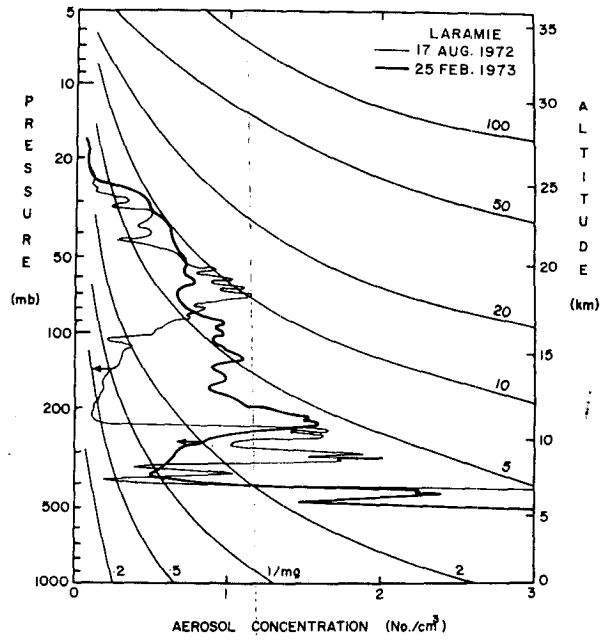

FIG. 9. Summer and winter aerosol concentration height profiles at Laramie, Wyo. The arrows mark the observed tropopause positions. The curved grid lines are lines of constant mixing ratio in units of particles per milligram of air.

just above the tropopause is more pronounced and one observes a considerable increase in the stratospheric particle loading below about 17 km during winter. Above this height the aerosol concentration remains relatively constant.

A useful parameter for studying the time variations of the aerosol is the area under the vertical concentration distributions. This integrated area is the total number of particles per unit area above the altitude at which the integration is begun. This quantity is shown plotted against time in units of 10^6 particles per cm^2-column above several different heights in the central box of Fig. 10. In each case the upper part of the sounding has been completed by extrapolating the observed concentration to zero at 10 mb pressure (31 km altitude). The uncertainties caused by this extrapolation are estimated to be less than a few percent and the overall flight-to-flight uncertainty of the integrated aerosol data is estimated to be $\pm 6\%$.

Except for an apparent increase at high altitude in early 1973, mentioned earlier in connection with the winter mixing ratio profiles, the greater than 20 km integration shows little time variation. Above 15 km, a late winter–early spring maximum begins to appear and is an obvious feature of the total aerosol loading above the tropopause, shown by the solid line in Fig. 10.

The observed tropopause heights are plotted in the upper portion of Fig. 10. The tropopause height was defined in the customary manner, i.e., the height of first attainment of a lapse rate $\leqslant -2°C\ km^{-1}$. An inverse correlation with the total aerosol loading above the

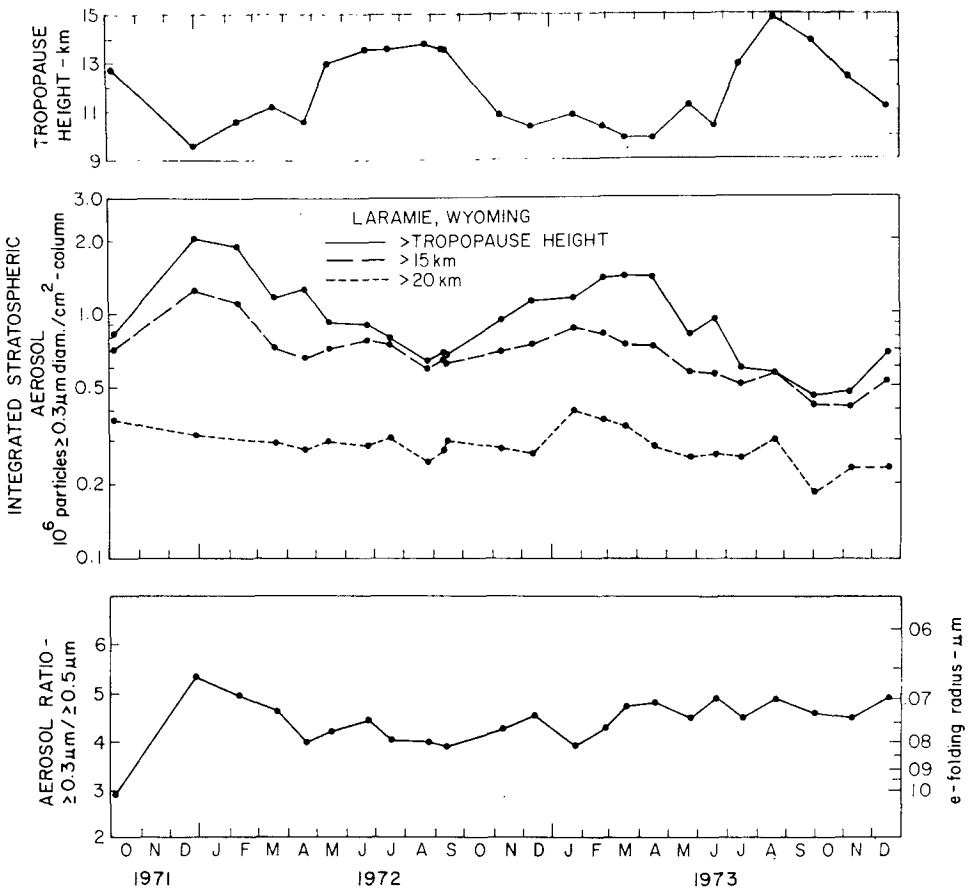

FIG. 10. Tropopause height, integrated aerosol, and aerosol ratio as a function of time at Laramie, Wyo.

tropopause is evident. In the lower portion of Fig. 10, the ratio of concentrations of the two sizes measured shows a uniformity in the size distribution at least beginning in early 1972. There is a suggestion of a long-term trend with the average concentration decreasing and the average particle size also decreasing. The long-term time constant (*e*-folding time) for the total aerosol is 3.3 years.

The excellent correlation of total stratospheric aerosol loading and tropopause pressure is demonstrated in Fig. 11. The effect of the apparent long-term variation is emphasized by separating the data into two time periods. The two straight lines are least-square fits to the data. The correlation coefficients are 0.93 for the first time period and 0.88 for the second. A similar high degree of correlation between total aerosol and tropopause height has been observed for all stations from which aerosol measurements were made during the program. This observation was reported earlier (Hofmann *et al.*, 1974).

6. Discussion

From the results of 24 aerosol soundings at Laramie during 1972 and 1973 it is possible to describe some of the characteristics of the stratospheric aerosol layer at northern midlatitudes during a relatively quiescent period in terms of volcanic activity. No volcanic eruptions violent enough to inject large amounts of material into the stratosphere have apparently occurred during this period of measurement, although such tropospheric events have occurred (Rosen *et al.*, 1972). The phenomenon of low-level volcanic activity generating gases which enter the stratosphere and form aerosol by chemical reaction cannot be ruled out.

Since on most occasions only two sizes are measured, only a crude indication of the character of the aerosol size distribution was obtained. However, the ratio of concentrations of the two sizes measured could be utilized to detect variations in size distribution. The aerosol found in the stratospheric layer during this period of measurement displayed a uniform size distribution, which resulted in a ratio of concentrations for the two sizes measured (greater than 0.3 and 0.5 μm diameter) of about 4–5. This gives a characteristic (*e*-folding) diameter of about 0.15 μm for an exponential size distribution or an exponent of about 3 for a power law integral size distribution. These conclusions would not change radically for other aerosol compositions if

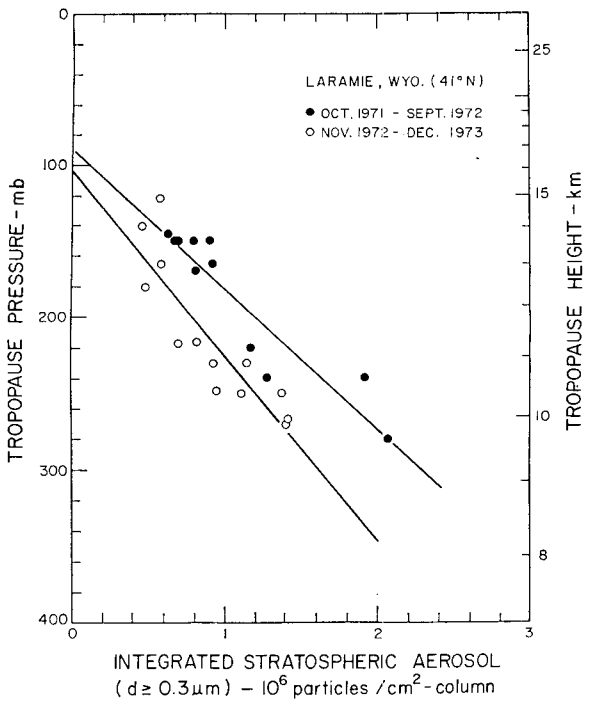

FIG. 11. The total stratospheric aerosol loading at Laramie as a function of observed tropopause pressure for two time periods. Straight lines are least-squares fit to the data for the two periods.

the aerosol remained nonabsorbing or nearly so. Substantial absorptive properties of the aerosol would result in a larger characteristic diameter or a smaller exponent for the same ratio of concentrations. These results assume spherical or nearly spherical shape and grossly nonspherical configurations would probably render these figures inappropriate.

The peak of the greater than 0.3 μm diameter aerosol mixing ratio, depending somewhat on season, is situated at a height of 18–22 km in northern midlatitudes. At the peak, the mixing ratios are about 8–10 particles per milligram of ambient air. This is equivalent to a mass mixing ratio of about 1.3 ppb. At the tropopause, the aerosol mixing ratio may be 10 times less, depending on season. In terms of particle concentration, the peak stratospheric values occur at altitudes about 4 km lower than the peak mixing ratios and have typically been in the range 0.5–1.5 cm^{-3} for the period of measurement.

The high degree of correlation between total stratospheric aerosol and tropopause height observed at Laramie and shown in Fig. 11 can hardly be coincidental. In fact, if one studies the individual profiles, it becomes evident that the variation occurs mainly in the lower stratosphere, i.e., that region in which the tropopause is exhibiting its seasonal variation in height. It is thus rather clear that, at least at northern midlatitudes, the tropopause height variation is affecting the stratospheric volume available for aerosol formation and transport. This effect is not observed above about 20 km. Also apparent in Fig. 11 is the effect of the long-term variation which causes the slope of the least-squares line fit to the aerosol loading vs tropopause height data to change.

The apparent ability of tropopause height variations to affect the aerosol loading by as much as a factor of 2, when such variations seem to have only small effects on the ozone distribution, can be attributed to the apparent location of the aerosol source region. The region of maximum aerosol mixing ratio is considerably closer to the tropopause than the ozone source region which is basically photochemically controlled and displays a maximum ozone mixing ratio at about 35 km in equatorial regions. Thus Dütsch (1963) observed an annual average correlation coefficient of only 0.5 between tropopause height and total ozone at Arosa, Switzerland. One concludes that the existence of significant aerosol concentrations in close proximity to the fluctuating tropopause gives the latter greater control over the "effective size" of the stratosphere in terms of aerosol capacity. If the stratospheric aerosol is formed from tropospheric SO_2 which penetrates the tropopause, as has been proposed (Junge, 1974), then one might expect a noticeable effect of tropopause motion on the Junge layer. However, no clear correlation between tropopause height and position of the layer of maximum mixing ratio has been observed at northern midlatitudes although, as will be shown in Part II, such a correlation appears to exist in equatorial and polar regions. This may suggest that the midlatitude aerosol profiles are predominantly determined by transport phenomena. However, the actual degree to which meridional transport and local production of aerosol

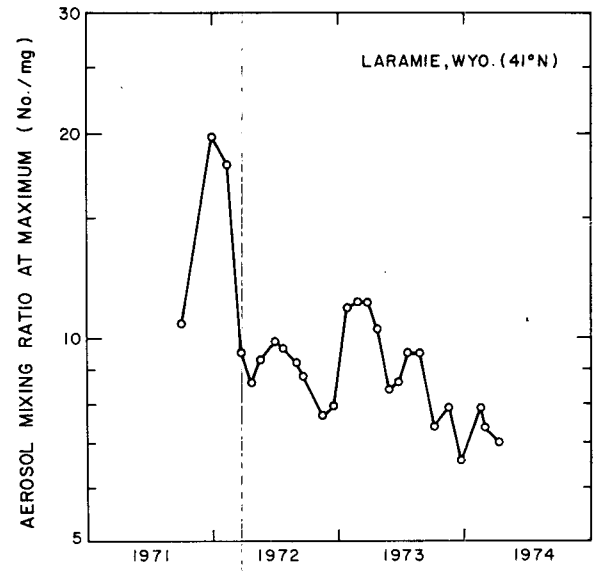

FIG. 12. Aerosol mixing ratio at the stratospheric maximum as a function of time at Laramie.

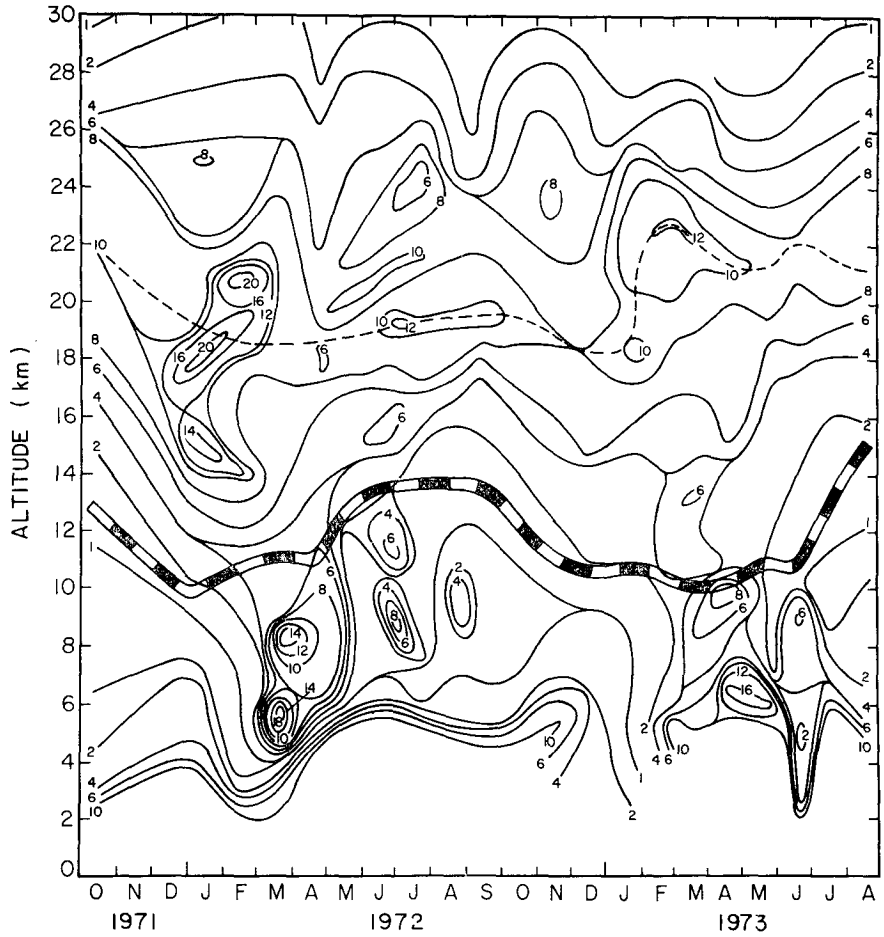

FIG. 13. Aerosol mixing ratio in units of particles per milligram of air as a function of height and time at Laramie. The observed height of the tropopause is indicated by the heavy broken line.

compete in producing the observed aerosol profile at mid and high latitudes is not yet known and can probably only be determined conclusively through model calculations when all the necessary data, including vertical distributions of SO_2 and Aitken nuclei, are obtained. In addition, the importance of interhemispheric exchange in the stratosphere will probably have to be taken into account to accurately describe the physical situation, e.g., such a process playing a sizable role could account for the observation of similar aerosol concentrations in the two polar regions (Hofmann *et al.*, 1973) when the Northern Hemisphere is the predominant anthropogenic sulphur producer.

The observation at Laramie of a highly layered aerosol structure in the region of the tropopause during spring and early summer when the total aerosol is decreasing suggests that horizontal transport, probably through the midlatitude tropopause gap, is the dominant sink mechanism in the lower stratosphere.

The nature of the apparent long-term variation is not well understood. It could be a consequence of a relatively high level of undetected volcanic activity which occurred in late 1971 and a dearth thereafter, combined with natural chemical formation, diffusion, sedimentation and coagulation. A possible volcanic candidate is Fuego in Guatemala (the same volcano which injected substantial material into the stratosphere in October 1974) which erupted 14–15 September 1971. All observers of the Fuego eruption in 1971 agreed that it was the most spectacular eruption of the last 70 years (Smithsonian Institution, 1971).

A parameter which may be better suited for identifying true long-term trends in the Junge layer itself is the aerosol mixing ratio at the maximum. This quantity does not appear to be overly sensitive to meteorological parameters and reflects what might be considered the source strength of particles. Fig. 12 shows the peak aerosol mixing ratios, taken from smoothed individual profiles, plotted against time for all soundings at Laramie through April 1974. Although the long-term trend is clearly visible in these data, it is complicated by rather large variations which do not lend themselves to

simple interpretation. They may be indicative of the amplitude of natural zonal fluctuations in the Junge layer itself; however, the high values in late 1971–early 1972 have not repeated themselves in the following two years and may represent a short-lived increase. The decreasing trend since early 1973 has been less complicated and exhibits an *e*-folding time of about 3 years, similar to the rate of decrease of the total aerosol.

The height of the maximum mixing ratio varies somewhat with time as is demonstrated in Fig. 13, where the aerosol mixing ratio, in units of particles per milligram air, is plotted vs height and time at Laramie. For example, the apparent mixing ratio increase in early 1973 occurred at a higher altitude than that in early 1972. Fig. 13 also suggests the existence of a complicated stratospheric-tropospheric exchange in spring. The lines of constant mixing ratio seem to follow the tropopause height in a general manner in the lower stratosphere (where tropopause effects are felt) but not at higher altitudes. The presence or absence of meridional transport during the winter buildup period is difficult to discern without similarly detailed histories at other latitudes to trace air parcel movements.

From this study one may conclude that the persistence of injections of material at altitudes below about 17 km in midlatitudes will depend on the season of injection, being influenced by seasonal fluctuations of the tropopause. The cleansing action takes place during spring and early summer so that a maximum lifetime of about nine months could be expected for late summer injections. Correspondingly short lifetimes (i.e., a few months) would be expected for winter injections. This is in general agreement with studies of the temporal behavior of stratospheric radioactive bomb debris (Machta and Telegadas, 1972). Above 20 km one cannot rely on this scrubbing mechanism and the lifetime of particulate matter is determined by diffusion, sedimentation and dynamic transport.

Acknowledgments. This research was supported by the Climatic Impact Assessment Program of the United States Department of Transportation through the Office of Naval Research and the National Science Foundation. We are indebted to the many members of the Atmospheric Research Group in the Department of Physics and Astronomy at the University of Wyoming who assisted in the instrument preparations, field work, and data reduction. A part of this analysis was done while one of us (DJH) was on leave at the Max Planck Institute for Aeronomy, Lindau/Harz, Federal Republic of Germany, and this opportunity as well as useful discussions there with Dr. P. G. Pruchniewicz are gratefully acknowledged.

REFERENCES

Bigg, E. K., A. Ono and W. J. Thompson, 1970: Aerosols at altitudes between 20 and 37 km. *Tellus*, **22**, 550–563.

——, Z. Kviz and W. J. Thompson, 1971: Electron microscope photographs of extraterrestrial particles. *Tellus*, **23**, 247–260.

——, and A. Ono, 1974: Size distribution and nature of stratospheric aerosols. *Proc. Intern. Conf. Structure, Composition and General Circulation of the Upper and Lower Atmospheres and Possible Anthropogenic Perturbations*, Melbourne, Australia, IAMAP Special Assembly, 14–25 January, p. 144.

Cadle, R. D., 1972: Composition of the stratospheric "sulphate" layer. *Trans. Amer. Geophys. Union*, **53**, 812–820.

Dütsch, H. U., 1963: Mittlewerte und wetterhafte Schwankungen des atmospharischen Ozongehalts in verschiedenen Höhen über Arosa. *Arch. Meteor. Geophys. Bioklim.*, **A13**, 167–185.

Hofmann, D. J., 1974: Stratospheric aerosol determinations. *Can. J. Chem.*, **52**, 1519.

——, J. M. Rosen, T. J. Pepin and R. G. Pinnick, 1973: Particles in the polar stratospheres. *Nature*, **245**, 369–371.

——, —— and ——, 1974: Influence of the tropopause height on the global stratospheric aerosol burden and implications for the recent increase in ozone. *J. Appl. Meteor.*, **13**, 734.

Junge, C. E., 1974: Sulfur budget of the stratospheric aeroso layer. *Proc. Intern. Conf. Structure, Composition and Genera Circulation of the Upper and Lower Atmospheres and Possible Anthropogenic Perturbations*, Melbourne, Australia, IAMAP Special Assembly, 14–25 January, p. 85.

——, C. W. Chagnon and J. E. Manson, 1961: Stratospheric aerosols. *J. Meteor.*, **18**, 81–108.

Lazrus, A. L., B. Gandrud and R. D. Cadle, 1971: Chemical composition of air filtration samples of the stratospheric sulfate layer. *J. Geophys. Res.*, **76**, 8083.

Machta, L., and K. Telegadas, 1972: Examples of stratospheric transport. *Proc. 2nd. Conf. Climatic Impact Assessment Program*, Washington, D. C., U. S. Dept. of Transportation, DOT-TSC-OST-73-4., p. 47.

Pinnick, R. G., J. M. Rosen and D. J. Hofmann, 1973: Measured light-scattering properties of individual aerosol particles compared to Mie scattering theory. *Appl. Opt.*, **12**, 37–41.

——, and D. J. Hofmann, 1973: Efficiency of light-scattering aerosol particle counters. *Appl. Opt.*, **12**, 2593–2597.

Rosen, J. M., 1964: The vertical distribution of dust to 30 km. *J. Geophys. Res.*, **69**, 4673–4676.

——, 1968: Simultaneous dust and ozone soundings over North and Central America. *J. Geophys. Res.*, **73**, 479–485.

——, 1969: Stratospheric dust and its relationship to the meteoric influx. *Space Sci. Rev.*, **9**, 58–89.

——, 1971: The boiling point of statospheric aerosols. *J. Appl. Meteor.*, **10**, 1044–1046.

——, 1972: The stratospheric aerosol background. *Preprints Intern. Conf. Aerospace and Aeronautical Meteorology*, Washington, D. C. Amer. Meteor. Soc., 205–208.

——, D. J. Hofmann, T. J. Pepin and J. Kroening, 1972: Extensive dust layer in the Northern Hemisphere. *Nature*, **240**, 347–348.

Smithsonian Institution, 1971: Annual Report, Office of Environmental Sciences, Center for Short-Lived Phenomena, Cambridge, Mass.